A Diffusion Tensor Imaging-Based Study on the Construction of Cortical-Hippocampal Fiber Pathways in Epileptic Mice

Lijun Zhang[1,2,a], Guanghao Zhang[1,2], Changzhe Wu[1,2], Xiaolin Huo[1,2], Shiji He[1,2], Jingxi Zhang[1,2], Cheng Zhang[1,2,b*]

[1]Institute of Electrical Engineering, Chinese Academy of Sciences, China
[2]University of Chinese Academy of Sciences, China

Abstract. OBJECTIVE This study investigated the structural connectivity between the prefrontal cortex (PFC) and hippocampus (HPC) in both normal and epileptic mice using diffusion tensor imaging (DTI) ,with a focus on the pattern of structural changes in the brain during the acute phase of epilepsy. METHODS Healthy male C57BL/6J mice (SPF grade) and epileptic mice induced by kainic acid (KA) injection *via* the tail vein were randomly assigned to the control group (NS, n = 5) and the epileptic group (KA, n = 5). The fractional anisotropy (FA), mean diffusivity (MD), and radial diffusivity (RD) values of both groups were compared and analyzed. Results from FA, MD, RD, and fiber tracking were also evaluated between the two groups. RESULTS (1) Diffusion tensor imaging findings: Compared to the NS group, the PFC-HPC pathways in the KA group showed varying degrees of FA reduction, with increases in both MD and RD. These differences were statistically significant ($P < 0.05$). (2) Distribution of fiber bundles across the whole brain: The total number of fiber bundles in the brains of NS and KA mice was 55,722 ± 3,798 and 50,969 ± 1,948, respectively, indicating a significant reduction in fiber count in the KA group ($P < 0.05$). (3) Region of interest (ROI) fiber bundle connectivity and distribution: The number of cortical-hippocampal fiber bundles in the NS and KA groups was 146 ± 39 and 70 ± 61, respectively. In the NS group, ROI connection sites were predominantly concentrated in the anterior and sublateral limbic regions of the PFC and the CA1 region of the HPC. In contrast, the KA group showed ROI connections primarily located in the prelimbic and sublimbic regions of the PFC and the dentate gyrus (DG) region of the hippocampus. CONCLUSION The present study successfully mapped the whole-brain fiber connectivity for both groups of mice. Compared to the NS group, the KA group exhibited significant reductions in fiber integration and connectivity, accompanied by myelin damage. These results suggest that the original PFC-HPC fiber pathway in the KA group was partially disrupted, with the potential generation of new fiber connections. Such alterations may contribute to the abnormal structural connectivity observed in the brain tissue of epileptic individuals.

1. Introduction

Epilepsy is a prevalent chronic neurological disorder, with temporal lobe epilepsy (TLE) being a common form of focal, drug-refractory epilepsy that continues to pose significant challenges in clinical diagnosis and treatment [1,2]. The pathophysiology of TLE is closely associated with deep brain tissue disorder [3], with hippocampal (HPC) lesions being among the most common causes of TLE [4-6]. TLE is typically characterized by recurrent seizures, often accompanied by sensory disturbances and altered consciousness [7], severely affecting the physical and mental health, as well as the quality of life of patients. Research has demonstrated that theta-gamma rhythm coupling between the hippocampus and prefrontal cortex (PFC) in both rodents and humans plays a pivotal role in emotion, consciousness, and memory [8], making it vital for the study of neural information transmission and processing.

Default mode network (DMN) is one of the major functional networks in the brain that maintains a high degree of functional connectivity between the cerebral cortex and deep brain regions (e.g., hippocampus) [9]. It suggests direct or indirect neuroanatomical connectivity between these brain regions to facilitate ongoing interbrain neuronal communication. It has been shown that epileptic activity in hubs can change functional connectivity between default networks [10,11]. However, the current research on DMN is more based on the functional connectivity between brain regions, and the neural fiber connections and projections of DMN are not yet fully understood.

Diffusion tensor imaging (DTI), based on diffusion-weighted imaging (DWI), quantifies the directional diffusion of water molecules by applying diffusion-sensitive gradient magnetic fields in multiple directions. This technique reflects the extent of white

[a]15138584420@163.com
[b*]Corresponding author: zhangchengcc@mail.iee.ac.cn

matter fiber tract damage [9]. DTI is a only non-invasive method capable of assessing the white matter fiber structure in vivo [12]. It can non-invasively assess the anatomical integrity of cerebral white matter fibers, fiber bundle density and connectivity through parameters such as FA, MD, RD, etc. DTI has proven essential for identifying epileptogenic foci in patients and guiding clinical decisions regarding surgical interventions [13]. Therefore, this study was designed to construct the neural fiber network of the mouse brain using DTI data, establishing the structural connections between cerebral cortex and hippocampus in both normal and epileptic mice. The study aims to investigate the structural changes in the mouse brain during the acute phase of epilepsy and explore their significance in the pathogenesis of the disorder.

2. Materials and methods

2.1. Experimental animals and groups

Healthy adult male C57BL/6J mice, SPF-grade (body weight 20-28 g, 7-9 weeks old), were purchased from Beijing Huafukang Bio-Technology Co., Ltd. [SCXK (Beijing) 2019-0008]. The mice were housed in cages (five mice per cage) at the Bioelectromagnetic Experimental Animal Center, Institute of Electrical Engineering, Chinese Academy of Sciences [SYXK (Beijing) 2022-0001]. A 12-hour light/dark cycle was maintained to simulate the natural circadian rhythm, with ad libitum access to food and water.

Kainic acid (KA) epilepsy was induced by intravenous injection of KA (16 mg/kg) in healthy male C57BL/6J mice. Five mice in the control group (NS, n = 5) and five in the epileptogenic group (KA, n = 5) were randomly assigned. Experiments were conducted during the daytime, from 8:00 to 18:00, in accordance with the approval granted by the Biomedical Research Ethics Review Committee of the Institute of Electrical Engineering, Chinese Academy of Sciences (Approval No. LL202404). All procedures adhered to the 3Rs principle of animal experimentation.

2.2. Magnetic resonance data acquisition

Magnetic resonance data were acquired using a Bruker 9.4T small animal MRI scanner (BioSpec 94/30/AV3HD USR, Bruker, Germany). DTI was performed using a single excitation spin-echo echo-planar imaging (SE-EPI) sequence with the following parameters: repetition time (TR) = 3200 ms, echo time (TE) = 33.8 ms, flip angle = 90°, field of view (FOV) = 40 × 40 mm2, matrix = 90 × 90 × 80, voxel size = 0.2 × 0.2 × 0.2 mm3, and a gradient sensitivity factor b-value of 800 s/mm2. A total of 34 volumes were acquired, including 4 b0 images with no gradient magnetic field (b = 0 s/mm2, repeated 4 times) for a scanning duration of 9 minutes 48 seconds. Image resolution was selected at 0.2 mm based on the optimal signal-to-noise ratio.

Data quality assurance primarily involved the verification of scanning parameters, such as TR, voxel size, and scanning duration, to ensure they are appropriate and consistent. Additionally, image artifacts, including distortions and other imperfections, were assessed. Other factors, such as head movement and the presence of image defects, were also examined. Ensuring high-quality data through rigorous quality checking is essential for obtaining more accurate and reliable results.

2.3. Data pre-processing

DTI data preprocessing was primarily conducted using FSL software [http://fsl.fmrib.ox.ac.uk/fsl/fslwiki/FSL]. In this study, the FDT module within FSL was employed for the processing of DTI data, following the procedure outlined below:

(1) Data format conversion: DTI data in DICOM format were converted into FSL-compatible 4D NIFTI files using the dcm2nii tool in MRICron.

(2) Eddy current and gradient direction correction: Artifacts resulting from eddy currents and gradient direction distortions, caused by coil currents during data acquisition, were corrected using the eddy_correct and fdt_rotate_bvecs tools in FSL, enhancing image quality.

(3) Extraction of the b0 image: The fslroi function was applied to extract the unweighted b0 image (with a b-value of 0) from any of the first four DTI volumes, which served as the reference image for further processing.

(4) Brain stripping: The RATS_MM tool was utilized to eliminate non-brain tissues such as the skull, maxillofacial regions, and neck, thus reducing computational load. Intensity thresholds were set between 1-3 for DTI and 20-25 for T2 images, generating both a binarized mask and an overlay image of the brain tissue. The stripping results were carefully examined by comparing the original and overlay images, with parameter adjustments and reprocessing applied when necessary to achieve optimal stripping.

(5) Reconstruction of diffusion parameter maps [14,15]: Fractional anisotropy (FA) and mean diffusivity (MD) images were reconstructed using the dtifit tool in FSL, while radial diffusivity (RD) images were calculated using the fslmaths function.

2.4. DTI-based nerve fiber tracking

Following the preprocessing of DTI images, the brain maps were aligned to individual Diffusion space based on Waxholm spatial mapping. The deterministic fiber tracking technique was applied to reconstruct the white matter fiber structure of the mouse brain, producing a comprehensive fiber distribution map. Regions of interest (ROIs), specifically the prefrontal cortex and hippocampus, were selected, and the nerve fiber bundles connecting these regions were identified and analyzed.

2.4.1 Image alignment

The image alignment process in this study primarily involves aligning brain maps to individual Diffusion space and subsequently extracting the ROIs from the indices of the standardized maps through the aligned brain maps, facilitated by T2 structural images of mice. This procedure utilizes the flirt and convert_xfm commands from the FSL software suite, and the specific steps are outlined as follows:

(1) Initially, the image in the individual Diffusion space (referred to as diff) is aligned with the image in the individual Structural space (referred to as struct), resulting in the transformation matrix diff2struct.mat.

(2) Next, the transformation matrix struct2diff.mat is derived by inverting the diff2struct.mat matrix, thus transforming the individual struct space to the individual diff space. This inverted matrix is employed to align the individual struct space to the individual diff space.

(3) Subsequently, the struct space image, now aligned with the diff space, is aligned with the standard space structural image (denoted as stand), yielding the transformation matrix diff2stand.mat.

(4) Finally, the transformation matrix diff2stand.mat is obtained by inverting the transformation matrix stand2diff.mat, which maps from the stand space to the individual diff space. The individual stand space atlas is then transformed into the individual diff space using nearest neighbor interpolation, resulting in the transformed brain atlas in the individual diff space.

2.4.2 Deterministic fiber tracing

Whole-brain fiber tracking and subsequent analysis were conducted using Diffusion Toolkit and TrackVis software. Initially, tensor calculations were performed with Diffusion Toolkit to derive the diffusion tensor and scalar metrics for each voxel across the entire brain, enabling whole-brain fiber connectivity analysis. This process required input of the corrected DTI image, b-values, gradient directions (input in (x, y, z) format for each row), and the number of b0s collected, among other parameters. The resulting output file was prefixed with "dti." Next, the Fiber Assignment by Continuous Tracking (FACT) algorithm was employed to reconstruct whole-brain neural fiber connections, with parameters set to an angular threshold of 60° and an FA threshold ranging from 0.1 to 1.0.

2.4.3 Fiber bundle-specific screening

ROIs were extracted using the Waxholm Spatial Atlas [16] to accurately isolate neural fiber connections traversing both the frontal cortex and hippocampus. The fslmaths command within the FSL software was utilized to extract other brain regions from the brain atlas that had been registered to the individual diffusion space. This study primarily focused on extracting the frontal cortex and hippocampal structures from the Index file. For extraction of additional brain regions, the same procedure was applied according to the corresponding brain region Index.

2.5 Statistical analysis

Statistical analyses were performed using SPSS 27.0 software. Diffusion parameter comparisons between the NS and KA groups were conducted *via* independent samples t-test, with data expressed as mean ± standard deviation (x ± s). A P-value of < 0.05 was considered statistically significant.

3. Results

3.1. Diffusion tensor results

Table 1 Diffusion parameters in the NS and KA groups (x ± s)

ROIs	Grouping	FA	MD ($\times10^{-4}$mm^2/s)	RD ($\times10^{-4}$mm^2/s)
PFC	NS	0.349 ± 0.039	7.746 ± 0.901	6.588 ± 0.616
	KA	0.244 ± 0.059*	9.340 ± 0.095*	7.550 ± 0.217*
HPC	NS	0.313 ± 0.040	8.402 ± 1.056	7.754 ± 1.164
	KA	0.281 ± 0.030	9.816 ± 0.122*	7.815 ± 0.610

Note. Compared with NS group, *P<0.05.

Table 1 presents the diffusion parameters and statistical analysis results for the NS and KA groups. Independent samples t-test analysis revealed that, compared to the NS group, all pathways between the prefrontal cortex and hippocampus in the KA group exhibited varying degrees of decreased FA and increased MD and RD. Significant changes ($P < 0.05$) were observed in the following pathways: a reduction in FA in the PFC pathway, along with increases in MD and RD; and an elevation in MD in the HPC pathway (Table 1).

3.2. Deterministic fiber tracking results

Figure 1 displays the outcomes of specific fiber tract screening for the NS and KA groups. As shown, ROI connectivity in the NS group was primarily concentrated in the prelimbic and the sublimbic regions of the prefrontal cortex and the CA1 area of the hippocampus. In contrast, the KA group demonstrated connectivity predominantly in the prelimbic and the sublimbic regions of the prefrontal cortex and the dentate gyrus (DG) area of the hippocampus.

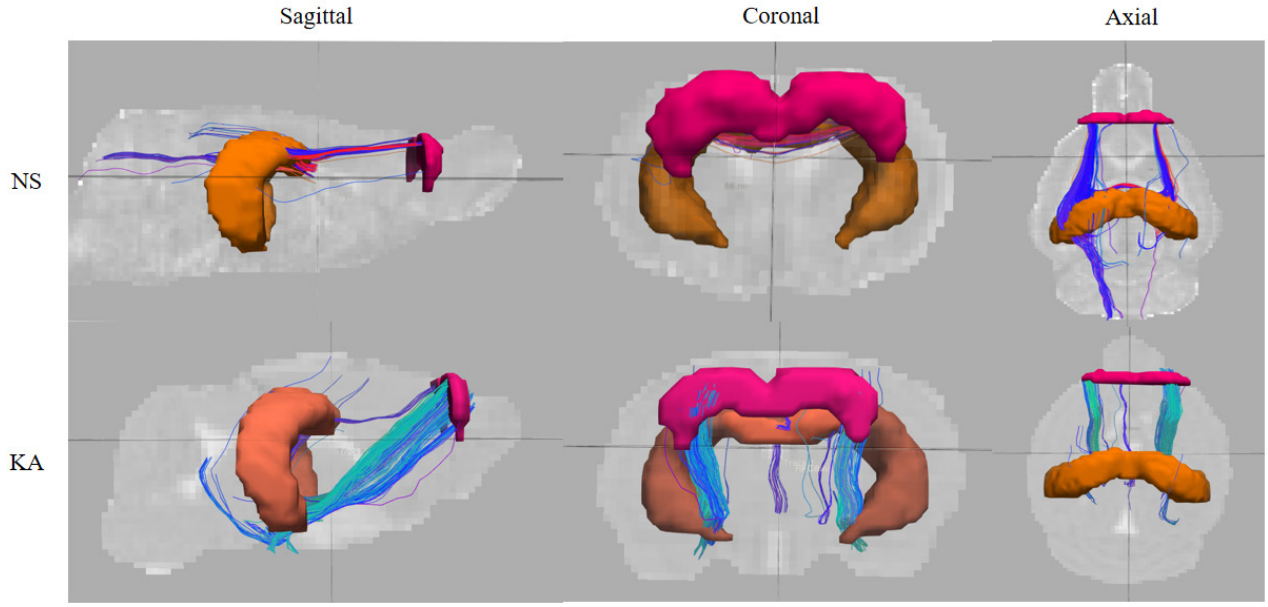

Fig.1 Results of specific fiber bundle screening in the NS and KA groups

The number and distribution of whole-brain and "PFC-HPC" (ROI) nerve fiber bundles in both groups were statistically analyzed using an independent samples t-test (Table 2). The results indicated that the total number of nerve fiber bundles in the whole brain was 55,722 ± 3,798 in the NS group and 50,969 ± 1,948 in the KA group, with a significant reduction in fiber count in the KA group ($P < 0.05$). The number of nerve fiber bundles in the PFC-HPC pathway was 146 ± 39 in the NS group and 70 ± 61 in the KA group, with no significant difference between the two groups.

Table 2 Results of fiber tracking in the two groups ($\bar{x} \pm s$)

	Grouping	Number of nerve fibers
Whole brain fiber tracts	NS	55722±3798
	KA	50969±1948*
"PFC-HPC" fiber bundles	NS	146±39
	KA	70±61

Note. Compared with NS group, *P<0.05.

4. Discussion and conclusions

DTI, a magnetic resonance imaging technique, exploits the directional diffusion of water molecules in myelinated nerve fibers, which is constrained by the myelin sheaths, allowing for non-invasive visualization of cerebral white matter fiber bundle orientations [17]. In this study, whole-brain fiber connections were successfully reconstructed for both normal mice and those in the acute phase of epilepsy, utilizing DTI data to reveal the functional pathways linking key brain regions (PFC and HPC). Preliminary findings indicate that structural connectivity between these critical regions was disrupted in the KA group, and the number of nerve fibers in the whole brain was significantly reduced ($P < 0.05$). The results suggest that the original fiber pathway between the cortex and hippocampus in KA group mice was partially compromised, with the potential formation of new fibrous connections. These alterations may underlie the abnormal structural connectivity observed in the brain tissue of epileptic subjects, contributing to impairments in self-regulation, memory retrieval, and related cognitive functions. In recent years, it has been shown that the total myelin number formation in the CA1 area of the cerebral cortex and hippocampal brain regions is reduced after epileptic seizures, whereas there is no significant change in the overall myelin formation and axonal damage in the DG area [18], and the result of the myelin reformation during seizures also promotes seizure reoccurrence, which affects the functioning of its pathologic circuits [19,20]. These findings are in general agreement with those of the current study in which the number of fibers in the whole brain was reduced and new fiber connectivity pathways were generated.

In the present study, multiple regions of altered diffusion tensor indices were observed in the cortex and hippocampus of epileptic mice, predominantly characterized by decreased FA and increased MD and RD. These parameter changes reflect the extent of neuronal histological damage. FA quantifies the degree of diffusion anisotropy in water molecules, with values ranging from 0 to 1. MD represents the overall diffusion level and resistance to diffusion, while RD measures the diffusion resistance perpendicular to the myelin sheath. Increased RD values suggest damage to the myelin sheath integrity. These parameters are commonly used to assess the anatomical integrity of white matter fibers, fiber bundle density, and connectivity. A reduction in FA and an increase in MD typically signal structural damage to brain white matter and a decline in the integration and connectivity of nerve fibers. In this study, compared to the NS group, the KA group exhibited varying degrees of decreased FA and increased MD and RD in the pathways connecting the PFC and HPC ($P < 0.05$). These results indicate a significant reduction in fiber integration and connectivity in the KA group's brain tissue, accompanied

by myelin damage. Previous studies have confirmed that epileptic seizures impair the integrity of cerebral white matter and delay myelin sheath formation, ultimately affecting nerve fiber integrity [21]. Salimeen et al. [21], in a study of 33 children with epilepsy using TBSS to analyze DTI data, found decreased FA and increased RD in epileptic children compared to controls ($P < 0.05$). Ercan et al. [22] also observed decreased FA values in the hippocampus, cingulate gyrus, and amygdala in patients with temporal lobe epilepsy. These findings align with those of the current study.

In this study, the fiber connections between the cerebral cortex and the hippocampal brain region in the DMN of mice were constructed based on DTI data using deterministic fiber tracing technique, which provides an experimental basis for the study of pathological changes in brain structure and the connection between brain structure and function. Meanwhile, the present study found that the DMN structure of epileptic mice may have generated new connections, which provides a new research idea for preoperative diagnosis of epileptic diseases and the selection of lesion sites for intraoperative treatment. However, there are still some limitations in the current study. Notably, the FA value tends to be lower when multiple fiber orientations are present within a single voxel, and tissue integrity degradation can also result in reduced FA values [23]. Consequently, the current study will continue to explore additional data and integrate multimodal approaches for a more comprehensive investigation. Moreover, given the small sample size in this study, further validation of the findings will be pursued by expanding the sample size in future research.

Acknowledgments

This study was supported by financial support from the National Key Research and Development Program of China (2022YFC2402201) and National Natural Science Foundation of China (No.52077209, 51977205). We are grateful to the technical staff in our lab and in the Institute of Automation, Chinese Academy of Sciences for assistance.

References

1. Borger, V., Hamed, M., Bahna, M., et al. (2022) Temporal lobe epilepsy surgery: Piriform cortex resection impacts seizure control in the long-term. Ann. Clin. Transl. Neur., 9: 1206-1211.
2. Banerjee, J., Srivastava, A., Sharma, D., et al. (2021) Differential regulation of excitatory synaptic transmission in the hippocampus and anterior temporal lobe by cyclin dependent kinase 5 (Cdk5) in mesial temporal lobe epilepsy with hippocampal sclerosis (MTLE-HS). doi: 10.1016/j.neulet.2021.136096.
3. Gleichgerrcht, E., Keller, S.S., Drane, D.L., et al. (2020) Temporal lobe epilepsy surgical outcomes can be inferred based on structural connectome hubs:a machine learning study. Ann. Neurol., 88: 970-983.
4. Colgin, L.L. (2016) Rhythms of the hippocampal network. Nat. Rev. Neurosci., 17: 239-249.
5. Connolly, M.J., Jiang, S.J., Samuel, L.C., et al. (2024) Seizure onset and offset pattern determine the entrainment of the cortex and substantia nigra in the nonhuman primate model of focal temporal lobe seizures. Plos. One., doi: 10.1371/journal.pone.0307906.
6. Sobstyl, M., Konopko, M., Wierzbicka, A., et al. (2024) Deep brain stimulation of hippocampus in treatment of refractory temporal lobe epilepsy. Neurol. Neurochir. Pol., 58: 393-404.
7. Fisher, R.S, Acevedo, C., Arzimanoglou, A., et al. (2014) ILAE Official Report: A practical clinical definition of epilepsy. Epilepsia., 55: 475-482.
8. Zheng, C.G., Colgin, L.L. (2015) Beta and gamma rhythms go with the flow. Neuron., 85: 236-237.
9. Zhou, Q., Zhang, G.H., Wu, C.Z., et al. (2022) Application progress of diffusion weighted magnetic resonance imaging in epilepsy. Magn. Reson. Imaging., 13: 104-108.
10. Park, K.M., Lee, B.I., Shin, K.J., et al. (2019) Pivotal role of subcortical structures as a network hub in focal epilepsy: Evidence from graph theoretical analysis based on diffusion-tensor imaging. J. Clin. Neurol., 15: 68-76.
11. Ikemoto, S., von Ellenrieder, N., Gotman, J. (2025) Interictal epileptiform discharge-related BOLD responses in the default mode network and subcortical regions. Clin. Neurophysiol., 170: 29-40.
12. Choi, E.B., Jang, S.H. (2020) Diffusion tensor imaging studies on recovery of injured optic radiation: minireview. Neural. Plast., doi: 10.1155/2020/8881224.
13. Tae, W.S., Ham, B.J., Pyun, S.B., et al. (2018) Current clinical applications of Diffusion-Tensor imaging in neurological disorders. J. Clin. Neurol., 14: 129-140.
14. Ota, Y., Shah, G.R. (2022) Imaging of normal brain aging. Neuroimag. Clin. N. Am., 32: 683-698.
15. Sun, S., Tian, M., Lin, X., et al. (2024) Disturbed white matter integrity on diffusion tensor imaging in young children with epilepsy. Clin. Radiol., 79: e119-e126.
16. Papp, E.A., Leergaard, T.B., Calabrese, E., et al. (2014) Waxholm Space atlas of the Sprague Dawley rat brain. Neuroimage., 97: 374-386.
17. Konomi, T., Fujiyoshi, K., Hikishima, K., et al. (2012) Conditions for quantitative evaluation of injured spinal cord by in vivo diffusion tensor imaging and tractography: Preclinical longitudinal study in common marmosets. Neuroimage., 63: 1841-1853.
18. Foutch, K., Tilton, I., Cooney, A., et al. (2025) Adolescent seizure impacts oligodendrocyte

maturation, neuronal-glial circuit Formation, and myelination in the mammalian forebrain. Neuroscience., 564: 144-159.

19. de Curtis, M., Garbelli, R., Uva, L. (2021) A hypothesis for the role of axon demyelination in seizure generation. Epilepsia., 62: 583-595.
20. Knowles, J.K., Xu, H., Soane, C., et al. (2022) Maladaptive myelination promotes generalized epilepsy progression. Nat. Neurosci., 25: 596-606.
21. Salimeen, M.S.A., Liu, C.C., Li, X.J., et al. (2021) Exploring variances of white matter integrity and the glymphatic system in simple febrile seizures and epilepsy. Front. Neurol., https://doi.org/10.3389/fneur.2021.595647.
22. Ercan, K., Gunbey, H.P., Bilir, E., et al. (2016) Comparative lateralizing ability of multimodality MRI in temporal lobe epilepsy. Dis. Markers., doi: 10.1155/2016/5923243.
23. Stasenko, A., Lin, C., Bonilha, L., et al. (2022) Neurobehavioral and clinical comorbidities in epilepsy: The role of white matter network disruption. Neuroscientist., 30: 105-131.